

# **RMBK SP-2 Validation Results (KS PH Rupture Simulation)**

**Bruce Schmitt  
Battelle, PNNL**

## ABSTRACT

The RELAP5 code has been developed for best estimate transient simulations of light water reactor coolant systems, during postulated accidents. Although developed and tested primarily for typical Western PWR and BWR reactor designs, the code is also being applied to safety assessments of Russian-designed reactors (RBMK and VVER reactors). This requires that the code be evaluated for transient phenomena specific to each reactor type. With the assistance of the United States Department of Energy (USDOE), through the Department's International Nuclear Safety Program, a project was established with the Russian International Nuclear Safety Center (RINSC) to address validation issues of the RELAP5 code. Through RINSC, with the participation of multiple Russian organizations, a process was initiated to identify and prioritize transient phenomena and experimental facilities with the purpose of defining standard problems that could be used to validate the RELAP5 code for application to RBMK and VVER reactors.

RBMK-SP2 was defined from a series of stop flow experiments that were performed with the KS facility. The KS facility is an electrically heated full-scale mockup of an RBMK fuel channel. Although the mockup is not an exact duplicate of an RBMK fuel channel, the heater bundle, lifting path (shield plug), steam water column (SWC) and upper drum are considered representative of an RBMK type fuel channel for the phenomena under investigation. The tests were designed to simulate the RBMK design-basis accident of a large header rupture at full power. That is, to simulate the abrupt flow stoppage that would occur following a rupture. Six of these experiments were selected for evaluation with the RELAP5 code. These experiments were performed to investigate the following phenomena important to RBMK safety:

- water release (ejection) from the fuel channel (FC) model and fuel simulator surface drying,
- dryout under sharp flow deceleration at the inlet of the RBMK-1000 and RBMK-1500 fuel assembly (FA) models,
- post dryout heat transfer and fuel simulator temperature conditions in the FA model under channel drying,
- steam and water counter current flows in the steam-water piping, and in the FC with the FA model,
- propagation of the reflood and quench front in the FA model under flow resumption at the channel inlet.

This report presents the results of calculations using the RELAP5/MOD3.2 code for the purpose of evaluating RELAP5's ability to simulate these phenomena. The overall results indicate that RELAP5 provided minimal or poor agreement with the test data.

## INTRODUCTION

RBMK Standard Problem 2 (SP2) was defined from a series of stop flow experiments that were performed with the KS facility to simulate the RBMK design-basis accident of a large header rupture at full power [1,2]. That is, to simulate the abrupt flow stoppage in the fuel channel (FC) that would occur following a rupture. Six of these experiments were selected for evaluation with the RELAP5/MOD3.2 code [3], ranging in heater power from 1.69MWth to 4.56MWth, with various initial coolant inlet temperatures, inlet flow rates and system pressures. Five of the experiments were performed with constant heater power and one experiment was performed with a variable power. The primary effort of the study was to evaluate the ability of RELAP5 to calculate rod bundle dryout and/or burn-out (critical heat flux) following the stoppage of flow and the subsequent rewetting after the flow was restored. Although intended to simulate a large header rupture (and the resulting loss of flow), the experiments did not involve system depressurization. In addition to dryout and rewet, the following phenomenon were investigated:

- water release (ejection) from the FC model and fuel simulator surface drying,
- dryout under sharp flow deceleration at the inlet of the RBMK-1000 and RBMK-1500 FA models,
- post dryout heat transfer and fuel simulator temperature conditions in the FA model under channel drying,
- steam and water counter-current flows in the steam-water piping, and in the FC with the FA model,
- propagation of the reflood and quench front in the FA model under flow resumption at the channel inlet.

The experiments were evaluated using the RELAP5/MOD3.2 code. This study was performed using this version of the code without any modifications [4]. The primary focus of the study was the evaluation of burn-out and rewet. However, additional insights could be obtained with respect to counter current flow and inter-phase drag. Because of the modeling similarities between RBMK-SP2 and the pilot study performed earlier, RBMK-SP1 [2,5] modeling options used in the previous study were also investigated for this study. This was primarily the use of the EPRI and modified Bestion bundle friction correlations (interfacial drag), and evaluating potential counter current flow in the SWC piping (liquid drainback to the bundle). In addition, sensitivity calculations were performed for time step size and heat structure nodalization. A total of 28 cases were run for the complete evaluation that is being documented for the RINSC program. This paper presents limited results from this study.

## FACILITY DESCRIPTION

The KS facility schematic is shown in Figure 1. The KS circuit simulates of the main structural elements of the RBMK reactor. From Figure 1, the main heater section used was 'Test Section 2', and the main flow path lines have been 'bolded'. The facility includes a distribution header (Lower header) and lower water communication line with an isolating control valve (2p). This piping connects to a heated channel (Test section 2), which contains an electrically heated bundle assembly. The heater bundle is an 18-pin assembly, and is surrounded by a talkoclorite insulator contained within the pressure tube. A riser with an internal shield plug, also called a lifting path, connects to the steam water communication (SWC) line leading to an upper header. A bypass line connecting the Lower and Upper headers, with control valve (4), effectively maintains constant differential pressure across the test section, even after inlet valve closure (2p). Figure 2 provides a simplified view of Test Section 2 between the Lower and Upper headers.

Additional equipment is provided that simulate the operation of the reactor steam drum separators, steam condensers, downcomer, and the main circulation pumps of the RBMK primary circuit. Depending upon the facility power level, heat can be removed through condensers and heat exchangers downstream of the separators (1K, 2K, 3K, 7T and 8T), and/or through heat exchangers connected directly to the Upper header (4T, 5T and 6T), as shown in Figure 1. Coolant is then collected in the intake header and returned to two circulation pumps connected in series and returned to the distribution header and test section. Additional bypass piping exists around the circulation pumps to maintain constant pump flow and head during the tests. A more detailed description of the facility can be obtained in [1].

Significant differences do exist between the KS facility and the RBMK reactor. Nitrogen pressurized accumulators provide overall pressure control in the KS facility. The steam drum is simulated by an upper header and three gravitation vertical separators (versus a single integral drum separator). In addition, the heater rod bundle was an 18 pin advanced bundle design versus the standard 18 pin bundle design. The lower bundle was representative of a standard RBMK-1000 fuel bundle while the upper bundle had enhanced grid spacers representative of a RBMK-1500 fuel bundle. Figure 3 shows the heater bundle arrangement, including the grid spacer arrangement. However, it was expected that the phenomena being investigated for an RBMK header rupture would be adequately simulated with the KS facility design and bundle configuration.

## DATA MEASUREMENTS

Although the entire KS circulation loop is simulated, only the experimental section of KS facility from the pressure header to the vertical separators is of interest to this evaluation, see Figure 2. Data measurements for the KS experiments were limited to this region. These measurements include the pressure tube inlet flow, four thermocouples for heater rod cladding temperature, one differential pressure reading across the heater bundle, and the heater bundle inlet pressure. Figure 2 shows the pressure tap and thermocouple elevations. Figure 3 shows the heater bundle rod cross-section and the associated thermocouples. Figure 4 is a detailed cross sectional view of the thermocouple location within a rod. Continuous data monitoring was provided for each of these instrument locations during each of the tests, except for Test-8. Test-8 was not able to monitor the bundle differential pressure measurement due to technical difficulties. A more detailed description of the instrumentation can be obtained in [1].

**Table 1) RELAP5 Model Equivalent Data Locations**

<b>Data</b>	<b>RELAP5 Model</b>	
<b>Thermocouples</b>	<b>HS</b>	<b>Volume</b>
TW-1	2102-59 mesh 8	210-58
TW-2	2102-58 mesh 8	210-57
TW-3	2101-33 mesh 8	210-32
TW-4	2102-10 mesh 8	210-09
<b>Pressure Taps</b>	<b>Volume</b>	
P4	210-57	
P16	210-02	

Table 1 provides a cross-reference between the data measurements and the equivalent locations in the RELAP5 model. Calculation results at these locations are compared against the corresponding measured data. The inner and outer heater rings are modeled separately in order to model the heater rod power distribution. Also, heat structures use 9 mesh points (8 intervals) for the base calculations. The depth of the thermocouple in the cladding from Figure 4 corresponds to the first inner mesh point from the rod surface (mesh point 8), and this is used for the temperature comparisons as opposed to the rod surface mesh point (mesh

point 9). The model nodalization scheme is presented in the next section. The temperature comparisons are presented in degrees K, and the differential pressures in Pa. The differential pressure is uncompensated for hydrostatic head (weight of the liquid between the taps), as indicated in the data report [1].

## MODEL DESCRIPTION

The RELAP5 model nodalization scheme is shown in Figure 6. The model simulates the entire cooling loop, using Test Section 2 for the heater bundle (Figure 1). Unless stated otherwise, all volumes are constructed using the BRANCH, PIPE or SINGVOL components in RELAP5. A control valve (SRVVLV option) was used to control the desired inlet flow rate for each test (inlet to vol. 110-01), for both the initial steady-state flow and transient flow response. The lower water line is volume 110 (01-07). These volume nodes are divided essentially at each pipe elbow, as the corresponding piping runs are of reasonable length (0.5m to 3.55m) and the region has low importance (does not require fine nodalization). The active heater bundle region is volume 210 (01-58), the upper and lower busbar connections (regions with copper rods) are volumes 200 and 220, respectively, and the pressure tube cap (dead-end region above the heater bundle) is volume 230. The active heater region was divided at 0.12m lengths (3 nodes between each major grid spacer) as this provided a convenient volume node length for the upper bundle region. The upper bundle contains the enhanced grid spacers representative of a RBMK-1500 bundle. The previous SP-1 analysis [5] for a different set of KS facility tests used heater node lengths of 0.25m. Node lengths of 0.12m was expected to yield better results during reflood (the SP-1 study did not examine reflood). The choice of 0.12m node lengths in the heater region was used as the reference size for determining the general node sizes in the remainder of the KS model. The general approach used was to limit the ratio of volume size in adjacent volumes to a factor less than 3/1, and to limit the ratio of volume size for any nodes that might be of importance to ~5/1 (compared to the heater region). Changes in adjacent volume sizes are limited to less than a factor of 10/1 (except at the large upper drum), as recommended in the RELAP5 code manuals.

The lifting path region is volumes 234 (01-03), 240 (01-07) and 250. Volume 234 is the pipe region below the shield plug, volume 240 is the annular shield plug and stringer assembly region, and volume 250 is the lifting path cap (dead-end region above the shield plug). Since the inlet elbow to the assembly is large relative to the pipe diameter, it is modeled as a volume equal to the arc-length of the elbow, at a 45° angle as opposed to connecting the lifting path as a 90°, vertical volume. The shield plug and stringer are modeled using the 'ANNULUS' option, although this is not expected to result in significant differences compared to a 'PIPE' volume as the region is unheated. The horizontal (slightly sloped) steam water communication line (SWC) is volume 300 (01-41). There are 40 nodes at the reference 0.72° slope, with the last node (node 41) modeling the 0.5m vertical rise to the upper drum. The steam water drum is volume 310 (01-18), and the uppermost SWC is volume 320 (01-07). The drum is divided into 18 nodes (uniform size) to limit the change in node size from the SWC (vol. 300), and to better capture the void distribution (stratification) along the header. The outlets from the upper drum (315 and 400) use the 'entrainment/pull through' option for the junction orientation.

The gravitation separators are lumped as a single unit, using four volumes, 330, 331, 332, and 335. This was done to allow for a recirculation flow path for the separator model within RELAP5 (vol. 335, SEPARTR option). This provided better steady-state solution stability as a simpler nodal scheme (with or without the separator model) tended to yield unwanted oscillations. The separator steam outlet, 600 (01-07), connects to the condenser, 610 (01-06), and the condensate outlet, 500 (01-07), connects to the after-cooler, 510 (01-06). The multipurpose inlet valves are modeled as servo valves (SRVVLV option). The secondary cooling sides, not shown, are modeled as u-tubes with constant inlet flow and temperature

boundary conditions. A downcomer line, 400 (01-08 and 420 (01-04), from the upper header returns a majority of the condensate directly to the intake header. The bypass heat exchanger is also modeled 440 (01-06). However, the test configuration did not require the use of this heat exchanger and so the inlet valve was modeled as closed. The condensate from the after-cooler is returned to the intake header, 700, while the condensate from the condenser is first combined with bypass flow from the upper header (at vol. 630), before returning to the intake header.

The nitrogen accumulators, 850 (01-10), are connected to the intake header via a surge line, 820 (01-06). The nitrogen receiver is also modeled, 853, and the associated vapor regions are initialized with nitrogen.

Condensate from the intake header is returned to the circulation pump suction, 720 (01-04), and then to the circulation pumps, 735 and 745. Both circulation pumps are modeled, and operate in series. The pump discharge piping, 750 (01-06), 755 and 760, returns condensate to the distribution header, 100, or to the pump bypass piping, 765 (01-00), 770, 775 (01-03) and 785 (01-04).

Pipe wall heat structures are modeled for the entire circuit. Heat loss to the environment is based on results from the SP-1 study [5]. An 'insulation' layer is modeled around the pipe walls and a constant sink temperature (40°C) applied at the boundary. An effective thermal conductivity of the insulation layer was determined based on the SP-1 study, set to match the given environmental heat loss. The heater bundle is modeled as two rings of pins (6 for the inner ring, and 12 for the outer ring). This was done to model the heater rod radial power distribution. The pressure tube heat structure also includes the talkoclorite insulator surrounding the heater bundle.

## TEST DESCRIPTION

Six experiments were chosen for evaluation with RELAP5/MOD3.2. Initial conditions for the experiments are presented Table 2. In each experiment the inlet control valve was closed to initiate the test, terminating flow to the channel and thus simulating the loss of flow that would occur following a large header rupture. After flow stoppage, liquid in the heater region begins a rapid boil-off and/or liquid expulsion. Within several seconds of valve closure, dryout occurs in the heater bundle and a rapid temperature excursion ensues. As the heater temperature approaches the heater rod design temperature limits, the inlet valve is reopened. The temperature excursion is thus terminated and quenching of the heater bundle occurs. Tests 4, 5, 6, 7 and 8 maintained constant heater power, and test 5' used a variable heating rate to simulate reactor shutdown.

The inlet control valve movement is not identical between the different cases. The time of initial movement (closing and opening) and the rate of movement are different in each case. The start time for closure and rate of closure were estimated from the data and the RELAP5 model valve movement set to closely match the data flow response. The start time for reopening and rate of opening were determined in a similar manner. A servo valve (SRVVLV option) was used with a table function that defined the valve position versus time to drive the valve position for each transient analysis. The valve position versus time was determined by manual iteration over several trial runs until the inlet flow response adequately matched the test data. Additional details of the conduct of the experiments can be obtained in [1].

The multipurpose valves between the separators and the condensers are assumed to be in a constant position during each experiment. System pressure is controlled by the accumulators and system dynamics. Steady state initialization of the RELAP5 model was achieved using these servo valves to 'throttle' the inlet flow to the condenser and after-cooler. After achieving steady state, the RELAP5 control schemes were bypassed and the valves maintained at constant positions as in the experiments. Typically, steady state conditions were achieved after approximately 1000 seconds. Heater bundle power is maintained constant in each test, except Test-5'. A table of power versus time was defined in the model for this case,

based on the experimental data. In all cases, the power profile has a flat axial power distribution.

**Table 2) KS Facility Initial Conditions**

No.	Experiment	Electrical power of fuel assembly model, MWth	Pressure at inlet of fuel assembly, P16, MPa	Water temperature at inlet of fuel channel, TF1, °K	Water flow rate at inlet GL, kg/s
1	Test-4	1.691	7.68	516.1	3.90
2	Test-5	2.486	8.40	527.4	4.70
3	Test-5'	2.532	7.95	533.1	4.17
4	Test-6	2.926	8.23	527.3	4.28
5	Test-7	3.488	8.23	529.3	4.13
6	Test-8	4.566	8.74	531.1	6.27

## DISCUSSION OF THE DATA

Examination of the test data indicated that there was an error in the differential pressure data. This conclusion was based on the differential pressure (dP16-4) measurements for the bundle. These are shown in Figures 33-38 (which compare the base calculations with the data). All of the experiments (except Test 8 which did not have data for this instrument) show that the heater bundle differential pressure holds constant at ~110,000 Pa, indicating that a significant quantity of water is remaining in the heater bundle. The analysis results indicate that insufficient liquid drain-back occurs to support such a high differential pressure, therefore the measurements are likely in error. This conclusion is consistent with the results of Standard Problem SP-1 [5], which indicated that liquid drain-back was severely limited at power levels of only 200kW, much lower than these experiments. Also, it is unlikely to be due to valve leakage, except for test case 8, as the required leakage flow rate would be excessively high (sufficient to prevent dryout). It is believed to be an instrument range error.

For the highest power case (Test-8) the cladding temperature response suggests that flow leakage is likely occurring after inlet valve closure and heater power is shutdown at approximately 11.4s. These were not indicated in the data report for the experiments. The conclusions are based on two observations in the data. First, TW-4 for the experiment does not show cladding dryout and TW-3 shows significant suppression in its temperature response when compared to the other experiments, which were conducted at lower powers. In addition, TW-1 and TW-2 show a slower cladding temperature heat-up rate following valve closure than the other experiments. Second, at ~11.4s the TW-3 and TW-4 temperature responses indicate a temperature drop below the initial cladding temperature. This is not seen in the other experiments. Also, even though flow has been reduced to below the initial level after 13s, cladding temperature and system pressure show a continuous decrease. This is consistent with an early reduction in power (and is estimated to have occurred at ~11.4s). In the calculation results presented for Test-8, valve leakage is assumed to have occurred (iterated to a 'best response' value), and shutdown is assumed to have occurred at ~11.4s.

## ANALYSIS RESULTS

A calculation matrix was established for this evaluation to examine the ability of RELAP5 to model these tests. The matrix was also designed to test several correlations available in RELAP5. This included testing the bundle friction correlation (EPRI versus Bestion correlation), liquid drainback from the SWC piping (by varying the junction hydraulic diameters), and evaluating the time step size and cladding heat structure mesh. The

matrix used is presented below in Table 3. Each of the six test cases was evaluated using a base model setup (designated ‘e’, which uses the EPRI bundle friction). In addition, based on the evaluation of the test data for case 8, valve leakage and an early shutdown were evaluated to determine a ‘best’ response. Sensitivity studies performed included time step size and heat structure mesh sensitivity analyses. However, a volume nodalization sensitivity study was not completed. Not all results from the matrix below are presented in this paper, although their impact to the analysis is included in the discussion. The results presented in this paper are indicated with an ‘x’ in the table. The results not presented are indicated with an ‘o’.

**Table 3) Calculation Matrix**

Test ID	Case Options							
	e	s	m	t	h	vp	b	
4	X	O	X	O	O		O	
5	X		X				O	
5'	X	O	X	O	O		O	
6	X		X				O	
7	X		X				O	
8	X	O	X	O	O	X	O	

**Case Option Definitions (x –results presented here, o –results not presented)**

- e** - EPRI bundle friction correlation (this is the ‘basecase’ model setup)
- s** - the SWC piping junction diameter is reduced by 1/8, based on SP-1 results [5] for liquid drainback
- m** - improved CHF multiplier coefficient, based on SP-1 results [5] for dryout prediction
- v** - valve leakage allowed
- p** - early power shutdown
- t** - time step size reduction
- h** - heat structure radial mesh reduction
- b** - Bestion bundle friction correlation

The predicted error in steady state differential pressure across the entire bundle is presented in Figure 7 for the ‘basecase’ results (‘e’ in Table 3). The predicted error increases smoothly, from –15% to +28%, when plotted against  $\Delta h/h_{fg}$  (change in enthalpy divided by heat of vaporization for the heated channel). This would indicate that the two-phase multiplier used within RELAP5 is not correctly capturing the RBMK pressure drop. Attempted variations in the wall roughness versus local form losses (the grid spacers) could not produce a significant improvement in the predicted error. The results using the Bestion bundle friction (not shown) yielded a similar steady state error prediction, even though the Bestion correlation predicts a significantly lower interfacial drag than the EPRI correlation. However, this similarity would be expected at these high mass flux levels. At high mass fluxes, the measured differential pressure should be dominated by wall friction and not interfacial drag and void distribution.

The predicted times to dryout are presented in Figure 8. The times to dryout are reasonably well predicted and follow the trend in the test data. However, this would be expected as the transients are essentially fast transients with rapid voiding in the bundle region. That is, an error in the predicted critical heat flux (CHF) limits would not have a significant impact on the time to dryout because CHF is reached very quickly. A slower transient or lower power condition might show greater variation (and in fact, this was seen in the SP-1 results [5] for lower bundle powers). Results using the Bestion bundle friction

correlation were also very similar for time to dryout (not shown). That is, no significant improvement in the results was seen. Again, even though the Bestion correlation predicts a lower interfacial drag than the EPRI correlation and more liquid is predicted in the bundle region for the steady state solution, the differences in results were minor.

The flow responses for each case are shown in Figures 9-14. The flow responses were effectively set to match the test data by iterating on the inlet valve opening and closing times. Thus reasonable agreement was obtained by ‘forcing’ the flow response. The thermocouple responses are shown in Figures 15-20. Reasonable agreement is seen in the initial time of dryout, rate of temperature rise, and in the peak cladding temperature. However, poor agreement is seen in the rewet. Only test cases 4 and 5’ predict cladding rewet after the inlet valve is re-opened for all of the thermocouples. In addition, the quench front shows an inversion where the lower elevation cladding stays in a post-dryout (CHF) condition and the upper elevation cladding shows partial rewet. Additional cases were run using an improved CHF multiplier for the RELAP5 Groenveld lookup tables (increasing the grid spacer CHF multiplier in the heat structure card). However, a large increase in the multiplier (from 0.5 to a value of 199.0) was required to obtain significant improvement. This is shown in Figures 21-26 for each test case. Each test case shows a more rounded rewet profile, consistent with the data, and cases 5 and 6 now show that rewet is predicted. However, test cases 7 and 8 still did not predict complete rewet, and the value used for the multiplier (199.0) does not have a basis. However, it does illustrate the potential improvement if a bundle specific correlation could be utilized.

The bundle inlet pressure responses are shown in Figures 27-32 and the bundle differential pressure responses are shown in Figures 33-38 (note: test case 8 did not have data available for this parameter). Overall, the trend in the pressure responses is matched relatively well. However, the magnitudes of the responses are poorly predicted. The magnitudes of the changes (high and low) in the inlet pressure are also poorly predicted. Investigation of the responses has not resulted in an explanation yet as to why the magnitudes of the responses are over-predicted. As noted in the discussion of the test data, the predicted bundle differential pressure responses show nearly complete voiding of the bundle and a corresponding low pressure differential. However, the test data consistently indicated a minimum differential pressure at ~110kPa. This was attributed to instrument range problems and not valve leakage, except for test case 8. In test case 8, it was concluded that some valve leakage was present (although this is not seen in the test report) and that an early power reduction occurred. A test case was run with valve leakage that provided a ‘best’ response and a power reduction (heater power turned off) at 11.4 seconds. The flow response for this case is included in Figure 39 with the basecase results. The inlet pressure response is included with the basecase results in Figure 40. Figure 41 shows the improved thermocouple responses. Without these corrections, the heater rods would not be predicted to rewet.

Results not presented or discussed here include the time step sensitivity study, the heat structure mesh sensitivity, and the investigation of the SWC liquid drainback. Briefly, the time step and heat structure studies showed no significant differences in the results for maximum time steps size limits between 0.01s and 0.001s, and heat structures meshes of 9 and 5 mesh points. The SWC investigation was for the junction hydraulic diameter, as this is used in the interfacial drag calculation in RELAP5. This was done to reduce the calculated counter-current flow based on the results of SP-1 [5]. That study showed excessive liquid drainback calculated at low bundle powers. Reducing the SWC junction diameters did not show any improvement in these results (which was expected as this would reduce cooling of the upper bundle from liquid drainback).

## CONCLUSIONS

Overall, the predicted responses for these test cases are considered minimal to poor. Although the flow responses were iterated to match the data reasonably well, significant discrepancies were seen in the steady state pressure drop and transient pressure responses. In addition, rewet was poorly predicted and, in some cases, not at all. Summarizing the conclusions:

- 1) The predicted steady state pressure drop in the heater bundle is not well correlated by RELAP5, and is considered to be minimally acceptable. The error plot of the calculated differential pressure suggests that the two-phase multiplier is under-predicted in the lower void fraction regions and over-predicted in the higher void fraction regions (and possibly mass flux dependent). This suggests that the RBMK bundle requires a more specific correlation than the Lockart-Martinelli correlation used in RELAP5 or that the mass-flux dependent coefficients be defined specific to the RBMK bundle.
- 2) Time to dryout is reasonably predicted for each case. However, this would be expected for even significant errors in the predicted CHF for this evaluation. These transients are relatively fast, resulting in a very rapid voiding in the bundle. A slower transient (flow reduction rate), or lower power condition, could be expected to yield larger discrepancies in the dryout condition if the predicted CHF has a large error.
- 3) RELAP5 consistently under-predicts rewet for the cases where power is maintained constant and the overall prediction is considered poor. In general this is in the conservative direction. However, for the case of power reduction, Test 5', early rewet is predicted. Sensitivity studies performed do indicate that an improved CHF correlation (specific to the RBMK fuel assemblies) would likely provide significant improvement. It should also be noted that for RELAP5/MOD3.2, the reflood model is disabled because of incompatibilities. Updated versions of RELAP5 with a reflood model may provide additional improvement as well.
- 4) Post-dryout heat transfer is reasonably predicted (except during rewet), as indicated by the rate of heatup in the cladding after dryout, and the peak cladding temperature is reasonably predicted. However, this is limited to conditions prior to reflood.
- 5) The progression of the quench front is not correctly predicted for all cases. In particular, the sequencing of temperature turn-over shows an inversion where the lower elevation cladding remains in post-dryout while the upper cladding is in partial rewet. Again, updated versions of RELAP5 with a reflood model may provide additional improvement.

## **6) REFERENCES**

- 1) "RBMK Type Reactor Core Thermal Hydraulic Processes Investigation Under Pressure Header Break Conditions ", Standard Problem INSCSP-R2 Definition, 1998.
- 2) "Final RELAP5 Validation Plan for Application to RBMK," Joint Project 6, International Nuclear Safety Center, 1998.
- 3) RELAP5/MOD3 Code Manual, NUREG/CR-5535, Vols. 1-5, 1995.
- 4) "Guidelines for Performing Code Validation Within the DOE International Nuclear Safety Center (INSC)," Joint Project 6, International Nuclear Safety Center, 1998.
- 5) Joint Project 6, "Comparison Report for INSCSP-R1," 1999.



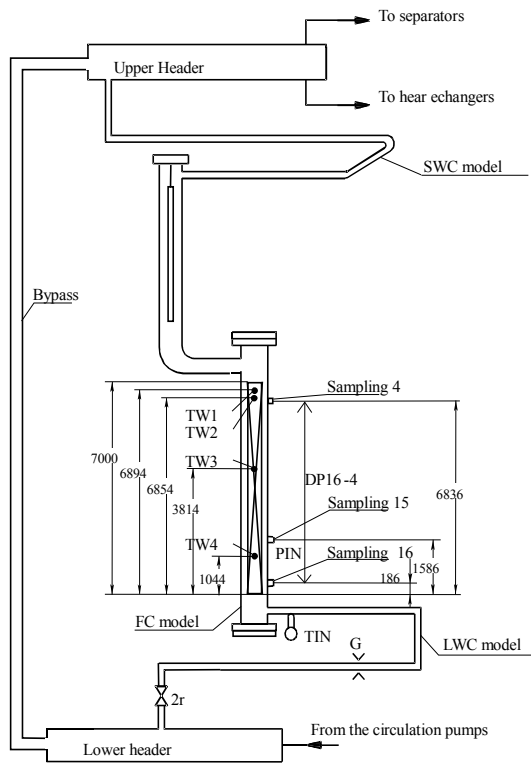


Figure 2) Test Section 2

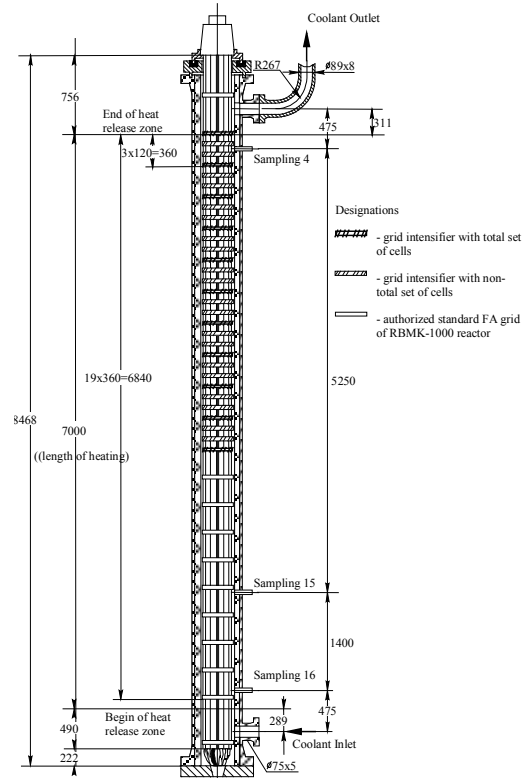


Figure 3) Heater Bundle Details

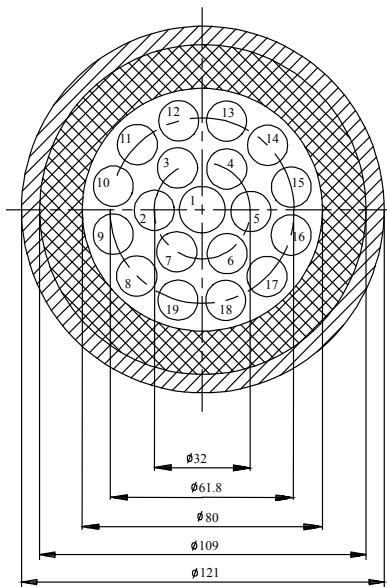


Figure 4) Heater Bundle Cross-Section

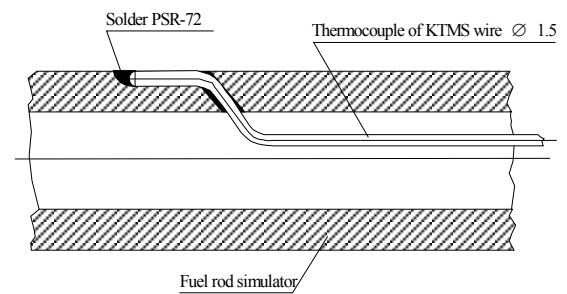


Figure 5) Thermocouple Location

Figure 6) KS Model Node Diagram

